JOURNAL OF THERMOPHYSICS AND HEAT TRANSFER
Vol. 8, No. 4, Oct.–Dec. 1994

Film Cooling Effectiveness in a Particle-Laden Flow

George J. Nacouzi*
TRW, Inc., San Bernardino, California 92402
and
Donald K. Edwards†
University of California, Irvine, Irvine, California 92717

A computational method is developed to evaluate the cooling effectiveness of a tangential slot in a particle-laden flow. The physical problem analyzed involves the tangential injection of a coolant at a wall subjected to convective heating from a turbulent boundary layer and radiative heating from hot particles. Previous published analyses did not include radiative or particle effects. The boundary-layer equations, including energy and species conservation, are solved using a finite difference scheme. The particle transport equation is also solved by a finite difference technique. A two-dimensional formulation for the solution of the radiative equation of transfer is developed using the spherical harmonics method. This formulation is different from those previously published in that it solves for an azimuthally integrated form of the intensity. This approach reduces the number of unknowns in the solution and is therefore more computationally efficient. Particle optical properties are obtained using the Mie scattering theory. A parametric study is performed to determine the effects of wall emissivity and other parameters on cooling effectiveness and particle deposition on the wall.

Nomenclature

a_n = complex size coefficients
b_n = complex size coefficients
C_p = specific heat at constant pressure, J/kg-K
c = mass fraction of freestream
D = mass diffusion coefficient, m²/s
d_p = particle diameter
G = mass fraction of particles
h = heat transfer coefficient, W/m²s
I = radiant intensity, W/m²-sr
I_b = blackbody intensity, W/m-sr
I^+ = intensity of the radiosity, W/m²-sr
I^- = intensity of the irradiation, W/m²-sr
i = $\sqrt{-1}$, also intensity function
k = thermal conductivity, W/m-s
k_e = extinction coefficient, 1/m
L = particle loading ratio
Nu = Nusselt number
P = pressure, N/m²
P_n^m = Legendre polynomial
Pr = Prandtl number
$\bar{p}$ = weighted phase function as defined by Eq. (22)
Q_{abs} = absorption efficiency
Q_{ext} = extinction efficiency
Q_{sca} = scattering efficiency
Q_v = volumetric heat flux, W/m³
q = heat flux, W/m²
q^+ = outgoing radiant flux, W/m²
q^- = incoming radiant flux, W/m²
Sc = Schmidt number
s = slot height
T = temperature, K
$TINF$ = freestream temperature
t = time, s
$UINF$ = freestream velocity
u = velocity in the streamwise direction, m/s
v = velocity in the normal direction, m/s
x = size parameter; also streamwise distance measured from slot exit plane, m
y = normal distance measured from the wall, m
$\tilde{(\ )}$ = mass or Favre averaged
ε = eddy viscosity, kg/m-s or emissivity
η = effectiveness defined by Eq. (28)
θ = zenith angle, rad
λ = wavelength, m
μ = viscosity, kg/m-s; also direction cosine
ρ = density, kg/m³; also reflectivity
T = optical depth defined by Eq. (8)
Φ = azimuthal angle, rad
Ω = solid angle, sr
ω = albedo for single scatter

Subscripts
c = coolant value
cool = coolant value
eff = effective
j = normal direction index
p = particle
T = turbulent
turbo = turbophoretic value
λ = evaluated at wavelength λ
0 = reference
1 = lower boundary, also freestream value
2 = upper boundary, also coolant value
∞ = freestream value

Received April 17, 1992; presented as Paper 92-4063 at the AIAA 1992 National Heat Transfer Conference, San Diego, CA, Aug. 9–12, 1992; revision received May 9, 1994; accepted for publication May 10, 1994.

*Section Head, Propulsion and Ordnance Department, Ballistic Missiles Division, P.O. Box 1310. Member AIAA.
†Professor of Mechanical Engineering. Fellow AIAA.

Introduction

PARTICLE radiation can be an important contributor to the heating of combustion chamber walls. The extent of the radiative contribution depends on many factors, such as the particle temperature, particle optical properties, and combustor wall optical properties. The analysis presented here considers alumina particles such as those found in a solid rocket motor.

New liquid propellants are being considered in which aluminum is injected along with the fuel into the combustion

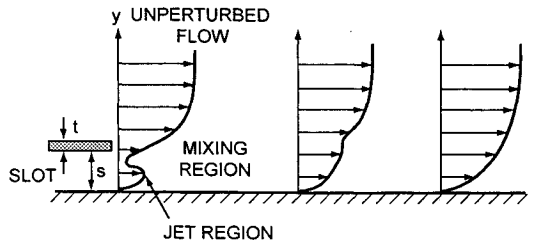

Fig. 1 Qualitative features of wall jet velocity development.

chamber. The aluminum reacts with the oxygen to form hot alumina particles that can be in either a liquid or solid state. These particles can significantly increase the heat load on the walls. This sharp increase can, in some cases, require special measures to cool the walls of the combustor. One successful approach used to cool hot surfaces is film cooling (Fig. 1). The present study examines the feasibility of film cooling a hot particle-laden flow. This analysis is performed using a finite difference approach to solve the relevant boundary-layer and mass transport equations, whereas the radiative equation of transfer is solved using a spherical harmonics or P-N method.

Film cooling has been experimentally investigated since the early 1960s. Seban and Back[1] and Samuel and Joubert[2] conducted experiments to determine velocity profiles of turbulent boundary layers downstream of tangential injections. In the 1970s numerical modeling of turbulent boundary layers with film injection was performed by Beckwith and Bushnell.[3] These workers developed a mixing length expression to account for turbulence. Cary[4] improved the turbulence model developed by the earlier workers and showed excellent agreement with experimental data. The particle concentration within the flow is solved using the approach developed by Reeks.[5] This author derived a particle transport equation for inhomogeneous turbulent flows, which is similar to Fick's law, but with an additional term—the turbophoretic or turbulent dispersion term—that provides for the transport of particles caused by inhomogeneous turbulence. The concentration of the injected coolant in the flow is calculated by solving the turbulent form of the species concentration equation. The eddy viscosity is calculated using the zonal method developed by Cary.[4] (The details of this calculation are given in the paper by Cary and are not repeated here.) The effects of particles on the flow turbulence is assumed to be negligible.

The radiative contribution to the wall heat flux is obtained by solving the equation of transfer for radiation (EOT) and coupling it to the flow energy equation.

Theory

The turbulent, steady-state, two-dimensional boundary-layer equations were developed using Favre averaging.[6] The continuity and momentum equations are given by

$$\frac{\partial}{\partial x}(\tilde{\rho}\tilde{u}) + \frac{\partial}{\partial y}(\tilde{\rho}\tilde{v}) = 0 \tag{1}$$

$$\frac{\partial}{\partial x}(\tilde{\rho}\tilde{u}\tilde{u}) + \frac{\partial}{\partial y}(\tilde{\rho}\tilde{v}\tilde{v}) = -\frac{\partial \bar{P}}{\partial x} + \frac{\partial}{\partial y}\left(\mu\frac{\partial \tilde{u}}{\partial y} - \rho u'v'\right) \tag{2}$$

$$\frac{\partial \bar{P}}{\partial y} = 0 \tag{3}$$

with boundary conditions given by

$$\begin{gathered}\tilde{u} = \tilde{v} = 0 \quad \text{at} \quad y = 0 \\ \tilde{u} = U_\infty \quad \text{and} \quad \tilde{v} = 0 \quad \text{at} \quad y = \delta\end{gathered} \tag{4}$$

An experimental study described by Rashidi[7] concluded that small heavy particles, at mass loading values similar to those used in this study, do not affect the fluid turbulent intensity. Therefore, it was assumed that particle effects on fluid turbulence is insignificant.

The energy equation was also developed using Reynolds decomposition along with Favre averaging. The general form of that equation can be found in Ref. 6.

The turbulent form of the species concentration equation was solved to obtain the concentration profile $\tilde{c}$ of the free-stream gas in the flow:

$$\tilde{\rho}\tilde{u}\frac{\partial \tilde{c}}{\partial x} + \tilde{\rho}\tilde{v}\frac{\partial \tilde{c}}{\partial y} = \frac{\partial}{\partial y}\left[\left(\frac{\mu}{Sc} + \frac{\varepsilon}{Sc_t}\right)\frac{\partial \tilde{c}}{\partial y}\right] \tag{5}$$

The boundary conditions for the above equation are simply given by

$$\tilde{c} = 1 \quad \text{at} \quad y = \delta \quad \text{and} \quad \frac{\partial \tilde{c}}{\partial y} = 0 \quad \text{at} \quad y = 0 \tag{6}$$

The one-dimensional EOT in Cartesian coordinate is given by[8]

$$\mu\frac{\partial I_\lambda}{\partial T_{y_\lambda}} = -I_\lambda + S_\lambda \tag{7}$$

where

$$T_\lambda(\text{optical depth}) = \int_0^s k_{e_\lambda}\, ds$$

$$S_\lambda(\text{source function}) = (1 - \omega_\lambda)I_{b_\lambda} + \frac{\omega_\lambda}{4\pi}\int_{4\pi} p(\Omega', \Omega)I_\lambda(s, \Omega')\, d\Omega' \tag{8}$$

The EOT is an integro-differential equation and cannot be solved by standard finite difference techniques. The method used in this study to solve the EOT is the spherical harmonics or P-N method, which involves representing the intensity by a series in spherical harmonics. The λ subscript accounting for the spectral dependency is dropped for clarity. Note that the analysis considered the radiation contribution from the particles only since the relative gas contribution was shown to be negligible by Babikian.[9] The radiation intensity can be represented by

$$I(T_y, \Omega) = \sum_{l=0}^{\infty}\sum_{m=-l}^{l} A_l^m(T_y)Y_l^m(\Omega) \tag{9}$$

where Y_l^m are the spherical harmonics, and A_l^m are the coefficients that need to be solved for. The details of the P-N method for the solution of the EOT are given by Osizik.[10] For the one-dimensional form of the EOT, the third-order spherical harmonics, or P-3, method yields four ordinary differential equations that are solved for simultaneously. The boundary conditions for these equations are obtained using Marshak's approach.

Given physical boundary conditions of the form

$$\begin{aligned}I^+(0, \mu) &= f_1(\mu) \\ I^-(T_0, \mu) &= f_2(\mu)\end{aligned} \tag{10}$$

The BCs for the P-3 solution are obtained by taking the moments of the above equations and integrating them over their appropriate range, i.e.,

$$\begin{aligned}\int_0^1 I^+(0, \mu)\mu^{2i-1}\, d\mu &= \int_0^1 f_1(\mu)\mu^{2i-1}\, d\mu \\ \int_{-1}^0 I^-(T_0, \mu)\mu^{2i-1}\, d\mu &= \int_{-1}^0 f_2(\mu)\mu^{2i-1}\, d\mu\end{aligned} \tag{11}$$

The equations for the four boundary conditions for an opaque wall with specified diffuse and specular reflectivities are developed in Appendix C of Nacouzi.[11]

The equation for particle mass concentration for an isotropic turbulent, isothermal flow is given by Rudinger[12] as

$$u_p \frac{\partial G_p}{\partial x} + v_p \frac{\partial G_p}{\partial y} = \frac{\partial}{\partial y}\left(D_p \frac{\partial G_p}{\partial y}\right) \tag{12}$$

In inhomogeneous turbulence, an additional transport phenomenon, in which particles are transported from high- to low-turbulence regions, needs to be accounted for. Reeks[5] performed a rigorous analysis of an inhomogeneous turbulent flow and developed a particle velocity term to account for the transport of particles down the turbulence gradient. This velocity term is given by

$$V_{\text{turbo}} = -t_p \frac{\mathrm{d}V_p'^2}{\mathrm{d}y} \tag{13}$$

where

$$t_p(\text{particle relaxation time}) = \rho_p \frac{d_p^2}{18\mu} \tag{14}$$

and V_p' is the particle fluctuating velocity.

Another particle transport mechanism that could be important when a high-temperature gradient exists within a flowfield is the thermophoretic transport. Im and Chung[13] reported success in accounting for this transport in a turbulent field by representing it by a velocity term given by

$$V_{\text{thermo}} = 2g(Kn)f(Kn)\frac{\partial T}{\partial y} \tag{15}$$

where $g(Kn)$ and $f(Kn)$ are correction factors given by the authors.

The particle temperature field is also calculated using a continuum approach. The particle energy equation is given by[14]

$$C_p G_p u_p \frac{\partial T_p}{\partial x} + C_p G_p v_p \frac{\partial T_p}{\partial y} = \eta_p A_p h(\tilde{T} - T_p) - \nabla \cdot q_r \tag{16}$$

With BCs given by

$$\begin{aligned} T_p &= T_\infty \quad \text{at} \quad y = \delta \\ T_p &= T_{\text{wall}} \quad \text{at} \quad y = 0 \end{aligned} \tag{17}$$

This form of the particle energy equation excludes any particle collision effects.

The particles are the main contributors to the attenuation and scattering of radiation. These effects are easily accounted for in the limiting cases of very small or very large particles, relative to the radiation wavelength. However, for intermediate-sized particles, the optical properties need to be calculated using Mie theory.[15] In the current study, the optical properties of the particle-laden flow are calculated using the exact solution of the Mie theory. The extinction and scattering efficiency factors are given by[15]

$$Q_{\text{ext}} = \frac{2}{x^2}\sum_{n=1}^{\infty}(2n+1)Re(a_n + b_n) \tag{18}$$

$$Q_{\text{sca}} = \frac{2}{x^2}\sum_{n=1}^{\infty}(2n+1)\{|a_n|^2 + |b_n|^2\} \tag{19}$$

where

$$x(\text{size parameter}) = (\pi d_p/\lambda) \tag{20}$$

The angular distribution or phase function is given by

$$f(\theta) = \frac{1}{4\pi}\sum_{n=0}^{\infty} f_n P_n(\cos\theta) \tag{21}$$

However, in order to reduce the computational time, an effective isotropic scattering coefficient $Q_{\text{sca,eff}}$ can be calculated. This effective coefficient is calculated by multiplying the value of Q_{sca} by a cosine weighted phase function $\tilde{p}$, where

$$\tilde{p} = \frac{1}{2}\int_{-1}^{1} f(\mu)(1-\mu)\,\mathrm{d}\mu \tag{22}$$

Then

$$Q_{\text{sca,eff}} = Q_{\text{sca}}\tilde{p} \tag{23}$$

This approach has been shown to yield very accurate results with an order of magnitude less computation time as compared to a full anisotropic solution.[11]

One of the parameters needed in the Mie calculation is the complex index of refraction of the particles. This value was obtained using the approach of Babikian,[9] in which the index of refraction of alumina is calculated as a function of temperature and wavelength.

Numerical Analysis

All the governing differential equations referred to are solved using an implicit finite difference approach. The equation of transfer for radiation is solved using the P-3 method. The code developed in this study was verified by comparing the results of the different subprograms to analytical and/or experimental data. A comparison of predicted velocity and temperature profiles with experimental values[2,16] is shown in Figs. 2 and 3. As can be seen in these figures, the comparison is good. Similar comparisons at different downstream stations were also performed and found to be of the same fidelity.

The particle transport algorithm was verified by calculating a particle concentration profile for a flat-plate turbulent flow. The results of that simulation, along with the results of an

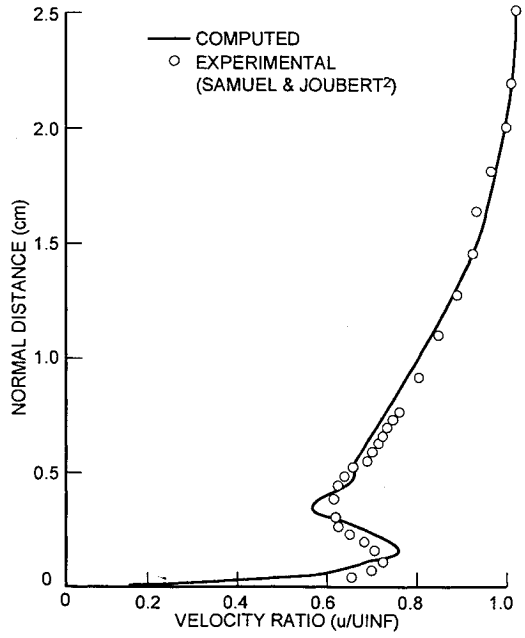

Fig. 2 Comparison of calculated velocity profile to experimental values at $x/s = 6.54$.

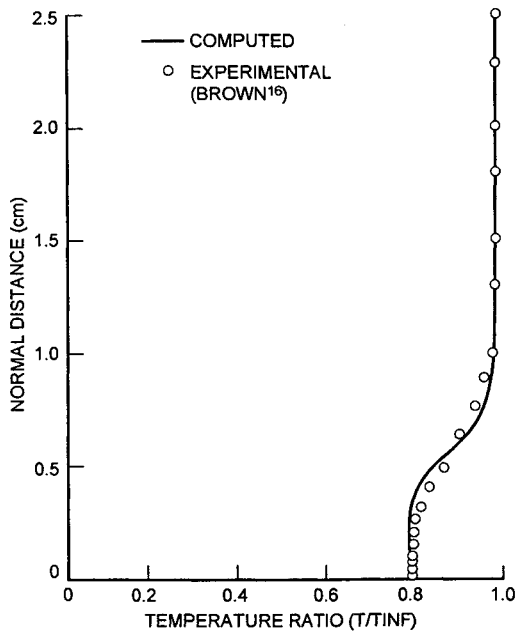

Fig. 3 Comparison of calculated temperature profile to experimental values at x/s = 15 for an adiabatic plate.

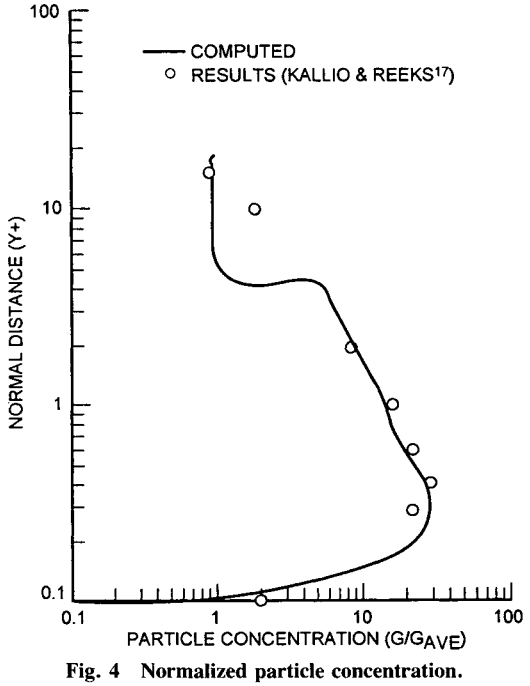

Fig. 4 Normalized particle concentration.

analysis performed by Kallio and Reeks[17] are shown in Fig. 4. Kallio and Reeks simulated the trajectories of thousands of particles using a Lagrangian tracking method. They also compared their results to other analyses. However, no experiment has yet been performed to determine the particle concentration in the viscous sublayer of a turbulent boundary-layer flow.

The P-3 algorithm used to solve the radiative equation of transfer was verified by comparing its results to exact solutions. As a test case, an isotropically scattering medium was considered with a linear profile for the blackbody intensity. The governing equations for a slab configuration are[18]

$$I^+(\mathrm{T}, \mu) = I^+(0, \mu)e^{-(t/\mu)} + \int_0^t S(t')e^{-[(t-t')/\mu]}\frac{\mathrm{d}t'}{\mu} \quad (24a)$$

$$I^-(\mathrm{T}, \mu) = I^-(t_0, -\mu)e^{(t-t_0)/\mu} - \int_t^{t_0} S(t')e^{-[(t-t')/\mu]}\frac{\mathrm{d}t'}{\mu} \quad (24b)$$

Table 1 Lower wall irradiation for linear I_b in a scattering medium

ω	P-3	Exact
0	24.72	24.74
0.15	25.10	25.07
0.50	26.10	25.96
0.70	26.76	26.57
0.90	27.49	27.26

where

$$S = (1 - \omega)I_b + \omega s' \quad (25a)$$

$$S' = \frac{1}{2}\int_0^1 I\,\mathrm{d}\mu \quad (25b)$$

The radiative flux on the lower wall was calculated for different values of the albedo ω by solving the above equations iteratively. The irradiation on the lower wall was also calculated using the P-3 approximation. The results for both methods are given in Table 1. The two methods yield results that are within 1.0% of each other; however, the iterative approach took two orders of magnitude more computer time than the P-3 calculations.

Results and Discussion

The effects of five different variables on the cooling effectiveness were investigated. Cooling effectiveness is defined as the ratio between the difference in wall and freestream temperature to the difference of the coolant and freestream temperature. The inclusion of cold particles in the injectant was also evaluated. The results presented in this analysis are based on the assumption of an adiabatic wall. This condition, which precludes the need for a wall conduction analysis, is given by

$$-k\left.\frac{\partial T}{\partial y}\right|_{y=0} + q_r|_{y=0} = 0 \quad (26)$$

It was also assumed that the particles transfer all their thermal energy to the wall upon impact. The freestream cloud emissivity, i.e., the upper boundary condition in the solution of the equation of transfer, is calculated using Chandrasekhar's[19] solution, which represents a cloud of infinite optical thickness and is given by

$$\varepsilon_\infty = (1 - \omega_\infty)^{1/2}H_H(\omega_\infty) \quad (27)$$

where ω is the albedo for single scatter of the freestream, and H_H is Chandrasekhar's H function.

The calculated adiabatic wall temperature T_w is transformed to an effectiveness η through the relation

$$\eta = \frac{T_\infty - T_w}{T_\infty - T_{\mathrm{cool}}} \quad (28)$$

Therefore, for a freestream temperature of 3000 K and an injectant temperature of 400 K, a value of η equal to 0.8 corresponds to a wall temperature of 920 K. In the cases which follow, effectiveness is plotted vs the streamwise distance x', where x' is the ratio of the distance from the slot exit plane x to the slot height s.

Reference Case

The first case considered, referred to as the base or reference case hereafter, is that of a gray wall with an emissivity of 0.25, a freestream temperature of 3000 K, and a coolant temperature of 400 K. The injectant and freestream velocities were taken to be 10 m/s, and a slot height of 2.0 mm was used. The initial velocity of the flow is given in Fig. 5. The

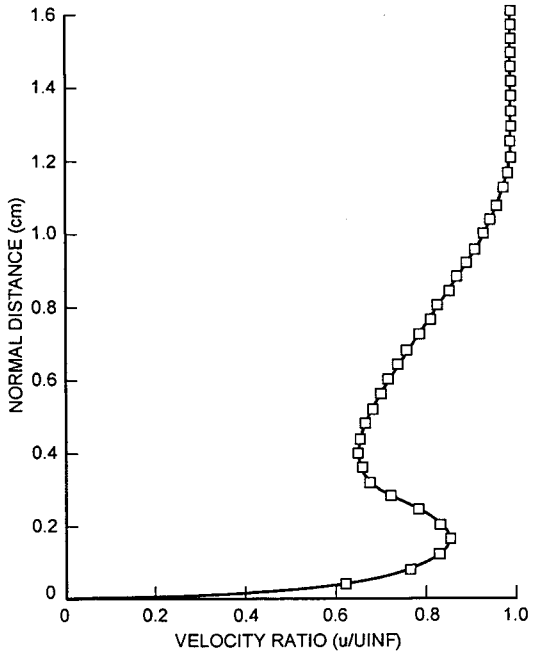

Fig. 5 Velocity profile for base case at $x/s = 10$.

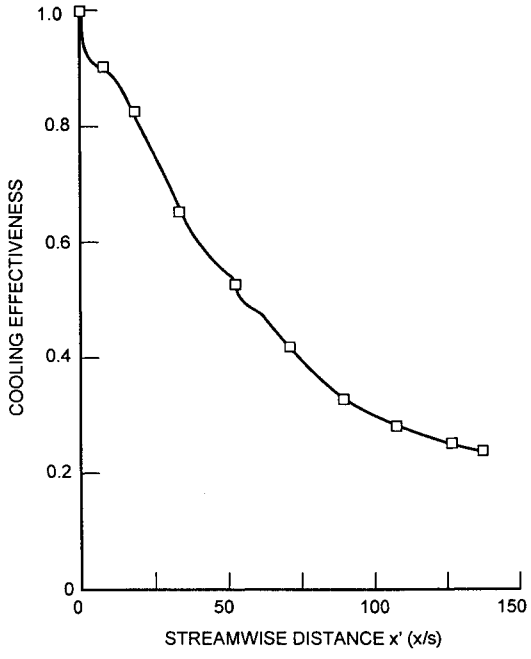

Fig. 6 Cooling effectiveness for base case ($\varepsilon = 0.25$).

particle loading (i.e., ratio of particle partial density to flow density) was set to 0.45 in the initial boundary layer with the film being free of any particles. A single particle size with a diameter of 15 μ was used.

The resulting effectiveness for the base case is shown in Fig. 6. A close examination of the effectiveness in this figure at x' between 5–15 reveals that the slope of η changes from an initially high (negative) value to a low value, then back again to a relatively high value. This peculiar behavior is due to the slot injection into the turbulent boundary-layer flow. A high-turbulence region exists where the mixing layer grazes the wall. This high region of turbulence results in a higher local Nusselt number and causes the wall to cool down. Also in this region, the particles tend to be ejected away from the wall due to the turbophoretic effect. The high turbulence region caused by the mixing layer grazing the wall has been experimentally verified[1,20]; however, no experimental evidence exists to verify or refute the particle behavior seen in this study. The value of the effectiveness reaches 0.75 around an x' of 25.

Radiation Effects

The importance of particle radiation on the cooling effectiveness was evaluated by considering a case in which radiation is neglected. A comparison of cooling effectiveness for the base case and the no radiation case is given in Fig. 7. The figure shows that, without radiation, the effectiveness falls slowly from 1.0 to 0.85 as the distance from the slot grows to 60 slot heights. However, when radiation is included, the effectiveness drops to below 0.8 in only 20 slot heights. Therefore, the radiation contribution significantly reduces the cooling effectiveness and cannot be neglected.

Wall Emissivity Effects

The effects of the wall emissivity ε on the cooling effectiveness η was investigated by varying ε from 0.1 to 1.0. The cooling effectiveness exhibits a very strong dependence on

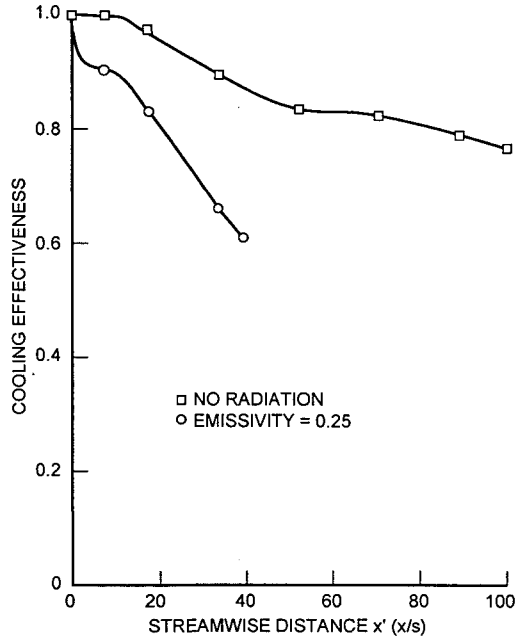

Fig. 7 Cooling effectiveness comparison between base case and no radiation case.

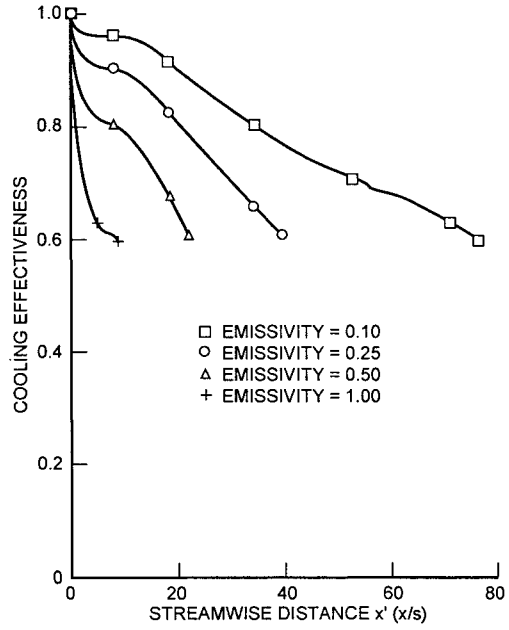

Fig. 8 Cooling effectiveness for different wall emissivities.

the wall emissivity, as shown in Fig. 8. This last figure shows that the cooling effectiveness for the black wall ($\varepsilon = 1.0$) drops to 0.6 within 10 slot heights. However, as the emissivity is reduced to 0.5, 0.25, and 0.1, the drop of η to a value of 0.6 is extended to 22, 45, and 80 slot heights, respectively. This calculation indicates that the selection of a wall material with a low emissivity can extend the effective cooling distance of a slot by a factor of two or more, depending on the maximum allowable wall temperature.

The effects of other parameters on the wall cooling effectiveness (i.e., particle adherence to the wall, freestream particle loading, spectral wall properties, freestream temperature as well as velocity, and coolant initial temperature and velocity) were investigated and are discussed in Ref. 11.

Conclusions and Recommendations

This study presents a computational method aimed at calculating the cooling effectiveness of a tangential slot in a particle-laden flow. All the important phenomena have been accounted for in the development of the model. Validation of the methodology was accomplished by checking the results of the various subprograms to exact solutions and experimental data.

A parametric study was conducted in order to understand the effects of different variables on the cooling effectiveness. The results showed that the radiative effects on film cooling effectiveness are very important and cannot be ignored. Also, it was found that wall emissivity is a key parameter in the overall design of the system and should be carefully considered. A low emissivity wall is very beneficial and greatly extends the effectiveness of a slot. As stated previously, other parameters were also investigated, but are not discussed in this article. A peculiar behavior of the particles was also noted in the region where the freestream intersects the wall. In this area of high turbulence it was found that the particles are ejected away from the wall region. This behavior is consistent with the turbophoretic phenomenon, but has not been verified experimentally.

In conclusion, the results presented herein indicate that the use of tangential slots in a particle-laden flow can be effective in cooling a hot wall. It should also be noted that in an actual application several slots would be placed in series along the wall. Since the downstream slots will have more benign initial conditions, their effectiveness will be higher than the first one. A study is currently underway to analyze the effectiveness of the downstream slots.

References

[1]Seban, R. A., and Back, L. H., "Effectiveness and Heat Transfer for a Turbulent Boundary Layer with Tangential Injection and Variable Free Stream Velocity," *Journal of Heat Transfer*, 84C, 1962, pp. 45–54.

[2]Samuel, A. E., and Joubert, P. N., "Film Cooling of an Adiabatic Flat Plate in Zero Pressure Gradient in the Presence of a Hot Mainstream and Cold Tangential Secondary Injection," *Journal of Heat Transfer*, Aug. 1965, pp. 409–418.

[3]Beckwith, I. E., and Bushnell, D. M., "Calculation by a Finite Difference Method of Supersonic Turbulent Boundary Layers with Tangential Injection," NASA TN-D6221, 1971.

[4]Cary, J. R., Bushnell, D. M., and Hefner, J. N., "Predicted Effects of Tangential Slot Injection on Turbulent Boundary Layer Flow over a Wide Speed Range," *Journal of Heat Transfer*, Vol. 101, 1979, pp. 699–704.

[5]Reeks, M. W., "The Transport of Discrete Particles in Inhomogeneous Turbulence," *Journal of Aerosol Sciences*, Vol. 14, 1983, pp. 729–739.

[6]Cebeci, T., and Smith, A., *Analysis of Turbulent Boundary Layers*, Academic Press, 1974.

[7]Rashidi, M., et al., "Particle-Turbulence Interaction in a Boundary Layer," *Journal of Multiphase Flow*, Vol. 16, 1990, pp. 935–949.

[8]Siegel, R., and Howell, J. R., *Thermal Radiation Heat Transfer*, Hemisphere, 1981.

[9]Babikian, D. S., "Experimental and Computational Studies of Volumetric Radiation," Ph.D. Dissertation, Univ. of California, Irvine, CA, 1989.

[10]Ozisik, M. N., *Radiative Transfer*, Wiley, New York, 1973.

[11]Nacouzi, G., "Radiative Effects on Film Cooling in a Particle-Laden Flow," Ph.D. Dissertation, Univ. of California, Irvine, CA, 1991.

[12]Rudinger, G., *Fundamentals of Gas-Particle Flow*, Elsevier, 1980.

[13]Im, K. H., and Chung, P. M., "Particulate Deposition from Turbulent Parallel Streams," *AIChE Journal*, Vol. 29, 1983, pp. 498–505.

[14]Azad, F. H., and Modest, M. F., "Combined Radiation and Convection in Absorbing, Emitting and Anisotropically Scattering Gas-Particulate Tube Flow," *International Journal of Heat and Mass Transfer*, Vol. 24, 1981, pp. 1681–1698.

[15]Van de Hulst, H. C., *Light Scattering by Small Particles*, Dover, New York, 1981.

[16]Brown, G. L., "Gas Film Cooling Past a Non-Adiabatic Flat Plate," Ph.D. Dissertation, Univ. of Idaho, Moscow, ID, 1969.

[17]Kallio, G. A., and Reeks, W. M., *International Journal of Multiphase Flow*, Vol. 15, 1989.

[18]Edwards, D. K., *Radiation Heat Transfer Notes*, Hemisphere, 1981.

[19]Chandrasekhar, S., *Radiative Transfer*, Dover, 1960.

[20]LaRue, J. C., and Libby, P. A., "Measurements in the Turbulent Boundary Layer with Slot Injection of Helium," *Physics of Fluids*, Vol. 20, No. 2, 1977, pp. 192–202.